Available online at www.sciencedirect.com
ScienceDirect
Thermochimica Acta 468 (2008) 81–86
thermochimica acta
www.elsevier.com/locate/tca

Mechanism for decomposition of aurichalcite—A controlled rate thermal analysis study

Veronika Vágvölgyi [a], Ashley Locke [b], Matthew Hales [b], János Kristóf [a], Ray L. Frost [b,*], Erzsébet Horváth [c], Wayde N. Martens [b]

[a] *Department of Analytical Chemistry, University of Pannonia, H8201 Veszprém, PO Box 158, Hungary*
[b] *Inorganic Materials Research Program, School of Physical and Chemical Sciences, Queensland University of Technology, 2 George Street, GPO Box 2434, Brisbane, Queensland 4001, Australia*
[c] *Department of Environmental Engineering and Chemical Technology, University of Pannonia, H8201 Veszprém, PO Box 158, Hungary*

Received 19 September 2007; received in revised form 28 November 2007; accepted 29 November 2007
Available online 5 December 2007

Abstract

Controlled rate thermal analysis (CRTA) of a series of synthetic aurichalcite $(Zn,Cu^{2+})_5(CO_3)_2(OH)_6$ with the ratio of Cu/Zn varying from 0.1 to 0.5 proves that the dehydroxylation and carbonate loss occur as non-isothermal and isothermal decompositions. The temperature of the thermal decomposition increases as the Cu/Zn ratio increases. Thermal decomposition of aurichalcite provides a method for preparing mixed oxide catalysts at the molecular level as opposed to the particle level.

CRTA technology enables separation of the processes of dehydration, dehydroxylation and decarbonation. X-ray diffraction of the products of the thermal decomposition proved to be a mixture of the oxides ZnO and Cu_2O.

Keywords: Aurichalcite; Catalysts; Mixed metal oxides; Dehydration; Dehydroxylation; Decarbonation; Controlled rate thermal analysis; CRTA

1. Introduction

The thermo-analytical studies of basic copper hydroxy-carbonates such as aurichalcite are not new, even though the first reported studies were in 1916 [1–5]. A similar lack of recent studies is true of minerals such as hydroxyzincite and hemimorphite [1–3,5–7]. There is a need to undertake a systematic study using the latest technology of carbonate and hydroxyl-carbonate minerals using thermo-analytical techniques including dynamic and controlled rate thermal analysis. Very few thermo-analytical and spectroscopic studies of the hydroxy carbonates have been forthcoming and what studies that are available are not new. Few Raman studies of any note are available [8,9]. To the best of the authors knowledge no thermo-analytical studies of aurichalcite have been undertaken, especially in recent times [1,4], although differential thermal analysis of some related minerals has been published [5]. The decomposition of aurichalcite results in the formation of a mixture of metal oxides of CuO and ZnO. Both these oxides may function as catalysts and photo-catalysts. The thermal activation of aurichalcite results in the formation of the oxide mixture, mixed at the molecular level and not at the particle level.

The mineral aurichalcite $(Zn,Cu^{2+})_5(CO_3)_2(OH)_6$ is one of a large number of highly coloured copper bearing minerals [5,10,11]. Aurichalcite forms in the oxidation zones of zinc–copper deposits. Crystals are grass green to pale blue-green [12], acicular and fibrous and often found in aggregates. Aurichalcite may be confused with rosasite minerals because of their similar appearance [13–16]. Rosasite minerals including glaukosphaerite; kolwezite; mcguinnessite are usually more massive and not lamellar [13]. Other related hydroxy carbonates are nullaginite and pokrovskite. It appears that aurichalcite is similar to hydrozincite and both minerals are formed under the same conditions when copper is present in the solution [17]. Williams further states that up to one quarter of the cation sites are occupied by Cu^{2+} [17].

In this work synthetic aurichalcite was prepared with wide variation in the Cu/Zn ratio. Greater concentrations of copper

* Corresponding author. Tel.: +61 7 3138 2407; fax: +61 7 3138 1804.
E-mail address: r.frost@qut.edu.au (R.L. Frost).

0040-6031/$ – see front matter © 2007 Elsevier B.V. All rights reserved.
doi:10.1016/j.tca.2007.11.024

normally give rise to other discrete phases such as malachite and rosasite. Interestingly the range of substitution of other transition metal ions in the hydrozincite lattice is very limited. The minerals in the hydroxy carbonate group have been synthesised because of their potential use as catalysts [11]. Further studies of synthetic hydroxyl-carbonates incorporated Al^{3+} into the structures [18]. Anthony et al. reports aurichalcite to be acicular crystals with prominent crystal growth along the [0 1 0] axis, commonly striated parallel to [0 0 1] axis. The mineral is of point group 2/*m* and space group $P2_1/m$ [19]. Based on the structure the symmetry of the carbonate anion is C_s. The accurate X-ray crystallography of aurichalcite is difficult to obtain because of its very small interwoven needles which makes obtaining single crystal studies difficult [5,19–21]. Harding showed the positions in the structure of aurichalcite are octahedrally coordinated. The atom positions occupied by zinc have tetrahedral coordination [21].

Recently thermogravimetric analysis has been applied to some complex mineral systems [22–35] and it is considered that TG-MS analysis may also be applicable to many carbonate minerals [26,36–40]. In this work we report the controlled rate thermal analysis (CRTA) of synthetic aurichalcite with variation in the Cu:Zn ratio.

2. Experimental

2.1. Synthesis of aurichalcite

The mineral $(Zn,Cu^{2+})_5(CO_3)_2(OH)_6$ was synthesised with different ratios of Cu to Zn. Williams inferred from studies of natural aurichalcite minerals that the highest ratio of Cu to Zn in aurichalcite is 1:3 [17]. A common formula for natural aurichalcite is $Cu_{1.25}Zn_{3.75}(CO_3)_2(OH)_6$. In this work aurichalcites were synthesised with a ratio of 0.1:0.9, 0.25:0.75, 0.4:0.6 and 0.5:0.5.

Synthesis of ideal products was modelled on the procedure by Fujita et al. [41]. A solution of metal ions (M^{2+}) was prepared by mixing appropriate concentrations of 1.5 M $Cu(NO_3)_2{\cdot}6H_2O$ and $Zn(NO_3)_2{\cdot}6H_2O$ that correspond to the desired metal concentrations desired in products. Synthesis of the lower copper concentrations of aurichalcite (Cu < 50%) was carried out by adding dropwise 100 cm^3 of a 1.5 M M^{2+} solution via a peristaltic pump to 1000 cm^3 of 0.2 M HCO_3^- solution at 338 K. The relatively sensitive nature of aurichalcite to acidic (pH < 6) conditions precluded the use of the depleting methods mentioned in the literature [42] in order to obtain optimum yields of high phase purity aurichalcite. As such, a stream of saturated sodium bicarbonate was added at a quasi-constant rate in order to maintain a pH ≈ 7.15, the samples were then aged for 30 min at 65 °C under constant stirring. Aged samples were vacuum filtered and washed with hot, degassed, demineralised water. Samples were then dried overnight at 100 °C.

2.2. X-ray diffraction

Powder X-ray diffraction analyses were performed on a Phillips X-ray diffractometer (radius: 173.0 mm). Incident X-ray radiation was produced from a long fine focused C-Tech PW1050 Co X-ray tube, operating at 40 kV and 32 mA. The incident beam passed through a 1° divergence slit, a 15 mm fixed mask and a 1° fixed anti scatter slit. After interaction with the sample, the diffracted beam was detected by a proportional detector with a 0.2 mm receiving slit fitted to a graphite post-diffraction monochrometer. The detector was set in scanning mode, with an active length of 2.022 mm. Samples were analysed utilising Bragg-Brentano geometry over a range of 3–75° 2θ with a step size of 0.02° 2θ, with each step measured for 200 s.

2.3. Thermal analysis

2.3.1. Dynamic experiment

Thermal decomposition of the synthetic aurichalcite was carried out in a Derivatograph PC type Thermoanalytical equipment (Hungarian Optical Works, Budapest, Hungary) capable of recording the thermogravimetric (TG), derivative thermogravimetric (DTG) and differential thermal analysis (DTA) curves simultaneously. The sample was heated in a ceramic crucible in static air atmosphere at a rate of 5 °C/min.

2.3.2. Controlled rate thermal analysis experiment

Thermal decomposition of the intercalated hydrotalcite was carried out in the Derivatograph under static air at a pre-set, constant decomposition rate of 0.1 mg/min. (Below this threshold value the samples were heated under dynamic conditions at a uniform rate of 1.0 °C/min). The samples were heated in an open ceramic crucible at a rate of 1.0 °C/min. With the quasi-isothermal, quasi-isobaric heating program of the instrument the furnace temperature was regulated precisely to provide a uniform rate of decomposition in the main decomposition stage.

3. Results and discussion

3.1. X-ray diffraction

The X-ray diffraction patterns for the synthesised aurichalcite together with two reference patterns are shown in Fig. 1. The XRD patterns for Cu/Zn aurichalcite from 0.1/0.9; 0.25/0.75, 0.4/0.6 and 0.5/0.5 are shown. No minor impurities are observed.

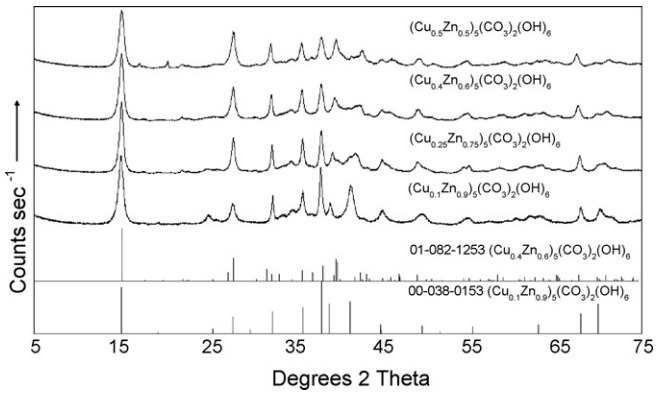

Fig. 1. XRD patterns of the synthetic aurichalcite and aurichalcite reference patterns.

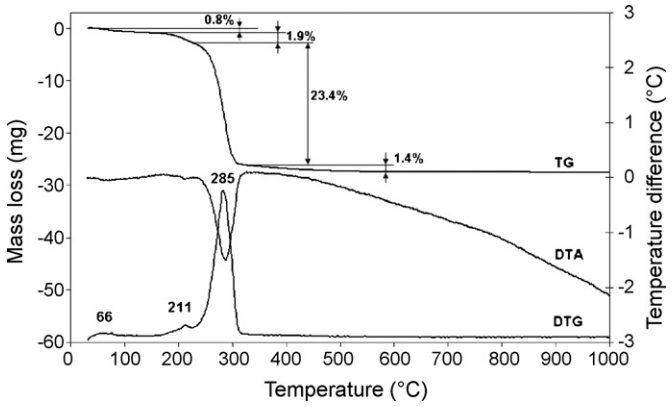

Fig. 2. The dynamic thermogravimetric and differential thermogravimetric analysis of aurichalcite with Cu/Zn ratio of 10:90.

Some variation in intensity of the XRD peaks is observed between the synthetic aurichalcites. This variation is related to the crystallinity of the synthetic aurichalcite. EDX analyses show that the average chemical composition corresponds to the formula given in Fig. 1.

3.1.1. Dynamic thermal analysis of aurichalcite(Cu/Zn 10/90)

The dynamic thermal analysis of aurichalcite with a Cu:Zn ratio of 10:90 is shown in Fig. 2. The Appropriate formula is $Cu_{0.5}Zn_{4.5}(CO_3)_2(OH)_6$. A sample mass of 103.00 mg was used in the experiment. A small mass loss of 0.80% was found in the TG plot at 66 °C. This mass loss is attributed to adsorbed water and the following reaction is envisaged:

$$Cu_{0.5}Zn_{4.5}(CO_3)_2(OH)_6{\cdot}xH_2O \rightarrow Cu_{0.5}Zn_{4.5}(CO_3)_2(OH)_6 + xH_2O$$

At 211 °C a mass loss of 1.9% is found and this mass according to mass spectrometric results may be accounted for by a loss of OH units. At 285 °C a mass loss of 23.4% is found. This corresponds to a theoretical mass loss of 24.0%. Thus all of the OH units and the carbonate are decomposed at this temperature according to the equation:

$$Cu_{0.5}Zn_{4.5}(CO_3)_2(OH)_6 \rightarrow 4.5ZnO + 0.5CuO + 3H_2O + 2CO_2$$

This result is supported by the DTA curve which shows a strong endotherm at 285 °C. A small mass loss of 1.40% occurs over the 350–1000 °C. It is noted that dehydroxylation and decarbonation occur in the dynamic experiment simultaneously.

In order to better resolve the decomposition processes above, controlled rate thermal analysis (CRTA) experiments were carried out as well in the same equipment using the CRTA control facility. In this case the decomposition of the mineral was carried out at a pre-set, constant, slow rate to provide time enough for the slow heat and mass transfer processes to occur. The essence of the technique lies in that each sample particle shall be heated under identical conditions. With the slow and constant decomposition rate of 0.10 mg/min the decomposition is carried out under quasi-isothermal, quasi-equilibrium conditions. This is achieved by the control of the furnace temperature regulated by the DTG signal through the computer.

3.1.2. Controlled rate thermal analysis of aurichalcite

The controlled rate thermal analysis of aurichalcite with Cu/Zn ratios of 10/90, 20/80, 40/60 and 50/50 are shown in Fig. 3a–d, respectively. The results of the CRTA analysis are reported in Table 1. Features are common to all of the CRTA patterns of aurichalcite: (a) a dehydration step at around 48 °C (b) a sharp non-isothermal dehydroxylation step at around 190 °C, (c) followed by a long isothermal decomposition step at around 233 °C and then (d) a decomposition at around 320 °C.

The results of the temperatures of thermal decomposition as a function of copper substitution are shown in Fig. 4. The first decomposition temperature remains constant within experimental error and is attributed to the loss of adsorbed water. An example of the calculations is given in Appendix A show that around 0.3 mol of water is associated with each synthetic aurichalcite. The values for the 10/90, 20/80, 40/60 and 50/50 are 0.31, 0.25, 0.38 and 0.42. The second decomposition step is attributed to dehydroxylation and the temperature varies from 190 to 250 °C. The third decomposition step assigned to the loss of both OH units and carbonate in an isothermal decomposition shows an increase in temperature as a function of the mole ratio of Cu. The observation of an isothermal step suggests that the intermediate compound is formed at the temperature of thermodynamic equilibrium at the pressure generated by the gases produced in the reaction in the close vicinity of the sample.

The reason for the increase in temperature with increasing Cu content is not known but is thought to be related to the crystallinity of the mineral. The fourth step, attributed to oxygen loss from CuO in the transformation to Cu_2O, shows a steady increase in temperature with increase in copper substitution. This non-isothermal step may be attributed to the decomposition of the metal oxide with oxygen evolution. Mass spectrometry of the aurichalcites shows that oxygen is lost at elevated temperatures around 780 °C. The temperature of the oxygen loss increases as the ratio of Cu:Zn increases. The temperature increases from 780 (10:90), 805 (20:80), 810 (40:60) and 815 (50:50). It is well known that ZnO decomposes or partially decomposes at elevated temperatures. It is also certain that CuO is reduced to Cu_2O or Cu at elevated temperatures. Thus the following reaction is envisaged:

$$CuO \rightarrow Cu_2O + 1/2O_2$$

X-ray diffraction of the products of the thermal decomposition of the aurichalcite is shown in Fig. 5. Included in figure of the decomposition product is the reference patterns of cuprite Cu_2O (01-078-2076) and zinc oxide (01-079-0206). Clearly the products of the thermal decomposition are ZnO and Cu_2O. Further it is known for hot stage Raman spectroscopy that these reactions listed above occur [43–49]. Raman spectroscopy shows that the formation of oxycarbonates does not occur as might be considered. It is apparent that the product of the thermal decomposition is a mixture of oxides as two separate phases and not an oxide with the two metals in the one oxide.

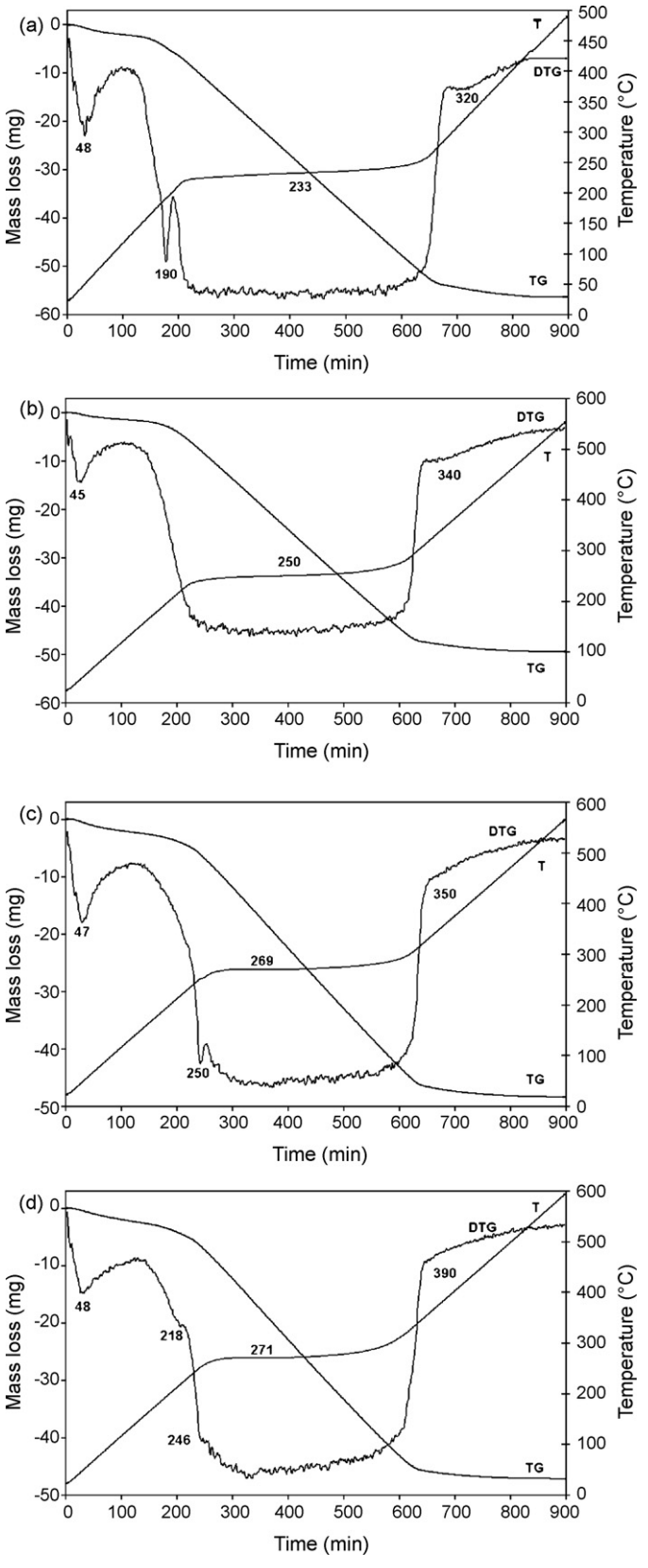

Fig. 3. (a) The controlled rate thermal analysis of aurichalcite with Cu/Zn ratio of 10:90. (b) The controlled rate thermal analysis of aurichalcite with Cu/Zn ratio of 20:80. (c) The controlled rate thermal analysis of aurichalcite with Cu/Zn ratio of 40:60. (d) The controlled rate thermal analysis of aurichalcite with Cu/Zn ratio of 50:50.

Table 1
Results of the CRTA analysis of aurichalcite with Cu/Zn ratios of 10/90, 20/80, 40/60, 50/50

Decomposition process	$(Cu_{0.1}Zn_{0.9})_5(CO_3)_2(OH)_6$		$(Cu_{0.2}Zn_{0.8})_5(CO_3)_2(OH)_6$		$(Cu_{0.25}Zn_{0.75})_5(CO_3)_2(OH)_6$		$(Cu_{0.4}Zn_{0.6})_5(CO_3)_2(OH)_6$		$(Cu_{0.5}Zn_{0.5})_5(CO_3)_2(OH)_{65}$	
	Temp. range (°C)	Mass loss (%)	Temp. range (°C)	Mass loss (%)	Temp. range (°C)	Mass loss (%)	Temp. range (°C)	Mass loss (%)	Temp. range (°C)	Mass loss (%)
Dehydration	23–125	1.0	24–126	0.8	25–118	1.2	23–131	1.2	23–142	1.4
Dehydroxylation	125–201	1.6					131–255	2.6	142–225	1.3
Dehydroxylation and decarbonation	201–289	23.2	126–311	25.0	118–329	25.0	255–332	22.3	225–349	23.6
Further decarbonation	289–478	1.1	311–547	1.1	329–568	1.0	332–561	1.0	349–589	0.8

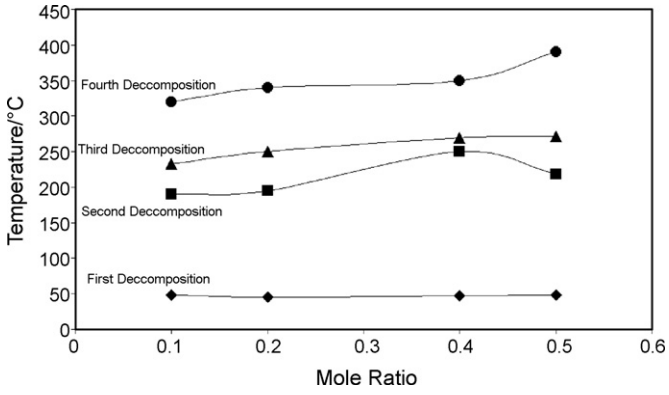

Fig. 4. Variation in the decomposition temperature with moles of copper.

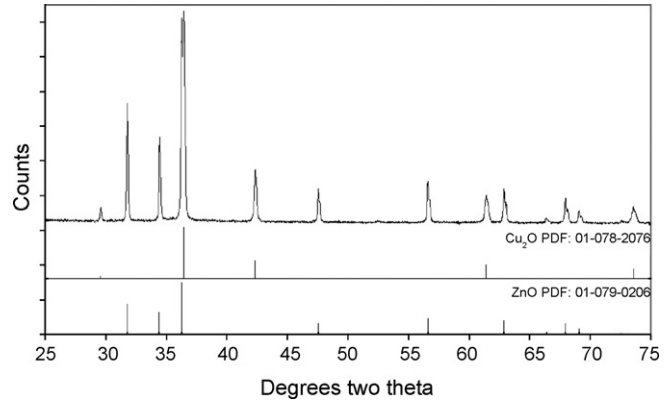

Fig. 5. X-ray diffraction patterns of the products of the thermal analysis.

4. Conclusions

Synthetic aurichalcite was prepared with variation of the Cu/Zn ratio from 0.1/0.9 to 0.5/0.5 [50]. The effect of increasing the Cu/Zn ratio results in an increase in the temperature of decomposition of the aurichalcite. This study is of importance in catalysis chemistry. Mixed Cu/Zn oxides can be prepared through the thermal decomposition of the synthetic aurichalcite. Thermal studies determine the temperatures to which the aurichalcite must be heated before decomposition or partial decomposition to the metals occur. The advantage of the thermal decomposition of aurichalcite is that it offers a mechanism for the preparation of the mixed metal oxides at the atomic level.

CRTA offers a better resolution and a more detailed interpretation of the decomposition processes via approaching equilibrium conditions of decomposition through the elimination of the slow transfer of heat to the sample as a controlling parameter on the process of decomposition. Constant-rate decomposition processes of non-isothermal nature reveal partial collapse of the layers, since in this cases a higher energy (higher temperature) is needed to drive out gaseous decomposition products through a decreasing space at a constant, pre-set rate. The CRTA experiment proves the thermal decomposition of aurichalcite with different Cu/Zn ratios is identical. The CRTA technology offers a mechanism for the study of the thermal decomposition of minerals such as the hydroxyl carbonate aurichalcite.

Acknowledgements

This research was supported by the Hungarian Scientific Research Fund (OTKA) under grant no. K62175. The financial and infrastructure support of the Queensland University of Technology Inorganic Materials Research Program is gratefully acknowledged.

Appendix A

Calculation of water content for $(Cu_{0.1}Zn_{0.9})_5(CO_3)_2(OH)_6$

Composition: $(Cu_{0.1}Zn_{0.9})_5(CO_3)_2(OH)_6 \cdot xH_2O$
Removing water up to 125 °C: 2.1 mg that is 0.117 mmol
Remaining dehydrated mineral up to 125 °C: 206.65 mg that is 0.377 mmol
Molar mass of dehydrated mineral: 548.17 g/mol

Calculation of x:
1 mol dehydrated mineral – x mol H_2O
0.377 mol dehydrated mineral – 0.117 mol H_2O
$x = 0.31$ mol

References

[1] C.W. Beck, Am. Mineral. 35 (1950) 985–1013.
[2] G. Cocco, Periodico di Mineralogia 20 (1951) 92–115.
[3] W.E. Ford, W.A. Bradley, Am. J. Sci. 42 (1916) 59–62.
[4] V.P. Ivanova, Zapiski Vserossiiskogo Mineralogicheskogo Obshchestva 90 (1961) 50–90.
[5] J.L. Jambor, Can. Mineral. 8 (1964) 92–108.
[6] F.L. Cuthbert, R.A. Rowland, Am. Mineral. 32 (1947) 111–116.
[7] W. Zabinski, Rocznik Polsk. Towarz. Geol. 26 (1957) 51–61.
[8] H. Fan, K. Tao, Y. Xie, K. Wang, Yanshi Xuebao 19 (2003) 169–172.
[9] W. Hong, S. He, S. Huang, Y. Wang, H. Hou, X. Zhu, Guangpuxue Yu Guangpu Fenxi 19 (1999) 546–549.
[10] R.S. Braithwaite, G. Ryback, Mineral. Mag. 33 (1963) 441–449.
[11] R.G. Herman, C.E. Bogdan, P.L. Kumler, D.M. Nuszkowski, Mater. Chem. Phys. 35 (1993) 233–239.
[12] B.J. Reddy, R.L. Frost, J. Near Infrared Spectrosc. 15 (2007) 115–121.
[13] R.L. Frost, J. Raman Spectrosc. 37 (2006) 910–921.
[14] R.L. Frost, D.L. Wain, W.N. Martens, B.J. Reddy, Polyhedron 26 (2007) 275–283.
[15] R.L. Frost, B.J. Reddy, D.L. Wain, W.N. Martens, Spectrochim. Acta A 66 (2007) 1075–1081.
[16] R.L. Frost, D.L. Wain, W.N. Martens, B.J. Reddy, Spectrochim. Acta A 66 (2007) 1068–1074.
[17] P.A. Williams, Oxide Zone Geochemistry, Ellis Horwood Ltd., Chichester, West Sussex, England, 1990.
[18] G. Sengupta, R.K. Sharma, V.B. Sharma, K.K. Mishra, M.L. Kundu, R.M. Sanyal, S. Dutta, J. Solid State Chem. 115 (1995) 204–207.
[19] J.W. Anthony, R.A. Bideaux, K.W. Bladh, M.C. Nichols, Handbook of Mineralogy, Mineral Data Publishing, Tiscon, Arizona, USA, 2003.
[20] Jambor J.L., MacGregor I.D., Paper Geological Survey of Canada, 74-1, Pt. B, 1974, 172–174.
[21] M.M. Harding, B.M. Kariuki, R. Cernik, G. Cressey, Acta Crystallograph., B: Struct. Sci. B50 (1994) 673–676.
[22] J.M. Bouzaid, R.L. Frost, A.W. Musumeci, W.N. Martens, J. Therm. Anal. Calorim. 86 (2006) 745–749.
[23] R.L. Frost, J.M. Bouzaid, A.W. Musumeci, J.T. Kloprogge, W.N. Martens, J. Therm. Anal. Calorim. 86 (2006) 437–441.
[24] R.L. Frost, Z. Ding, Thermochim. Acta 397 (2003) 119–128.
[25] R.L. Frost, Z. Ding, Thermochim. Acta 405 (2003) 207–218.
[26] R.L. Frost, Z. Ding, H.D. Ruan, J. Therm. Anal. Calorim. 71 (2003) 783–797.

[27] R.L. Frost, K.L. Erickson, M.L. Weier, A.R. McKinnon, P.A. Williams, P. Leverett, Thermochim. Acta 427 (2005) 167–170.
[28] R.L. Frost, J. Kristof, W.N. Martens, M.L. Weier, E. Horvath, J. Therm. Anal. Calorim. 83 (2006) 675–679.
[29] R.L. Frost, W. Martens, M.O. Adebajo, J. Therm. Anal. Calorim. 81 (2005) 351–355.
[30] R.L. Frost, D.L. Wain, R.-A. Wills, A. Musemeci, W. Martens, Thermochim. Acta 443 (2006) 56–61.
[31] R.L. Frost, M.L. Weier, Thermochim. Acta 409 (2004) 79–85.
[32] R.L. Frost, M.L. Weier, Thermochim. Acta 406 (2003) 221–232.
[33] R.L. Frost, M.L. Weier, W. Martens, J. Therm. Anal. Calorim. 82 (2005) 373–381.
[34] R.L. Frost, R.-A. Wills, J.T. Kloprogge, W. Martens, J. Therm. Anal. Calorim. 84 (2006) 489–496.
[35] R.L. Frost, R.-A. Wills, J.T. Kloprogge, W.N. Martens, J. Therm. Anal. Calorim. 83 (2006) 213–218.
[36] R.L. Frost, K.L. Erickson, J. Therm. Anal. Calorim. 76 (2004) 217–225.
[37] R.L. Frost, K. Erickson, M. Weier, J. Therm. Anal. Calorim. 77 (2004) 851–861.
[38] R.L. Frost, M.L. Weier, K.L. Erickson, J. Therm. Anal. Calorim. 76 (2004) 1025–1033.
[39] R.L. Frost, M.L. Weier, J. Therm. Anal. Calorim. 75 (2004) 277–291.
[40] R.L. Frost, W. Martens, Z. Ding, J.T. Kloprogge, J. Therm. Anal. Calorim. 71 (2003) 429–438.
[41] S.-I. Fujita, Y. Kanamori, A.M. Satriyo, N. Takezawa, Catal. Today 45 (1998) 241–244.
[42] G.J. Millar, I.H. Holm, P.J.R. Uwins, J. Drennan, J. Chem. Soc., Faraday Trans. 94 (1998) 593–600.
[43] R.L. Frost, J.M. Bouzaid, J. Raman Spectrosc. 38 (2007) 873–879.
[44] R.L. Frost, J. Cejka, G.A. Ayoko, M.L. Weier, J. Raman Spectrosc. 38 (2007) 1311–1319.
[45] R.L. Frost, J. Cejka, M.L. Weier, W.N. Martens, G.A. Ayoko, J. Raman Spectrosc. 38 (2007) 398–409.
[46] R.L. Frost, M.J. Dickfos, J. Raman Spectrosc. 38 (2007) 1516–1522.
[47] A.J. Locke, W.N. Martens, R.L. Frost, J. Raman Spectrosc. 38 (2007) 1429–1435.
[48] R.L. Frost, M.L. Weier, W.N. Martens, J.T. Kloprogge, J. Kristof, J. Raman Spectrosc. 36 (2005) 797–805.
[49] R.L. Frost, M.L. Weier, J. Raman Spectrosc. 35 (2004) 299–307.
[50] G.-C. Shen, S.-i. Fujita, S. Matsumoto, N. Takezawa, J. Mol. Catal. A: Chem. 124 (1997) 123–136.